# MODELING OF METAL TRANSFER IN GAS METAL ARC WELDING

Yong-Seog Kim and T. W. Eagar
Massachusetts Institute of Technology

## ABSTRACT

The droplet size is predicted using both the static force balance theory and the pinch instability theory as a function of welding current. Experimental measurements of the droplet size are also presented. The causes for the deviation of predicted droplet size from measured size is discussed with suggestions for modifications of the theories in order to more accurately model metal transfer in GMAW.

Edison Welding Institute Annual North American Welding Research Seminar, Columbus, OH, 1988

## 1.0 INTRODUCTION

Since introduction of the gas metal arc process in the late 1940s, it has become one of the most important welding processes which often constitutes a major fraction of the product cost of large structures. It is now used in joining most commercial alloys, however, many applications of the process are still limited by a lack of understanding of the physics and the ability to control the process. For example, the heat flow and the mass flow processes are understood only generally and a detailed knowledge of what occurs in the arc is lacking. Heat flow in the system determines the melting behavior of the base metal and the electrode, while mass flow controls the shape of the weld pool and the metal transfer from the electrode. Among these phenomena, metal transfer is of great importance because it is crucial in controlling the process.

Table 1 shows the classes of metal transfer as defined by the International Institute of Welding (IIW). These include short circuit, globular and spray metal transfer. Short circuit metal transfer occurs when a metal drop bridges the weld pool. It is used for welding sheet metal which requires very shallow penetration. The globular and spray transfer modes are employed in heavy section welding and are used most generally. The globular transfer mode is loosely defined as occurring when the drop diameter is two to three times the diameter of the electrode. It is more difficult to define spray transfer since there are three different types: projected transfer, streaming transfer and rotating transfer. In projected transfer, the drop diameter is about the same size as the diameter of the electrode. This mode is generally very stable. In streaming transfer, the drop is formed at the tapered tip of the electrode and the size of the droplets is as fine as 0.1 times the electrode diameter. Rotating transfer occurs at very high welding currents when the liquid string rotates in the welding arc, spraying tiny liquid drops in an uncontrolled manner. This transfer mode is very unstable and sets practical upper limits on the power input into the system.

In GMAW, globular metal transfer occurs at low welding currents while spray transfer occurs at relatively higher welding currents. The transition from globular transfer to spray transfer as the welding current increases has been reported to be very sharp as shown in Figure 1 (Ref. 1). According to this figure, as welding current is increased, the drop transfer rate and the size of the drop suddenly changes at a critical current.

### 1.1 Theories of Metal Transfer Mechanism

A number of theories has been proposed to explain metal transfer mechanisms. These include the static force balance theory (Refs. 2, 4), the pinch instability theory (Refs. 5, 6), the plasma force theory (Ref. 7), and the critical velocity theory (Ref. 8).

Among these theories, the plasma force theory and the critical velocity theory are proposed to explain the transition of metal transfer from globular transfer to spray transfer.

In the static force theory, four kinds of forces are considered: viz., the gravitational force, the electromagnetic force, the plasma drag force, and the surface tension force. According to this theory, the molten drop is removed from the electrode when the holding force of the surface tension is exceeded by the sum of the detaching forces.

$$F_g + F_{em} + F_d = F_s \tag{1}$$

where $F_g$ is the gravitational force which is equal to the drop mass times the acceleration of gravity. $F_{em}$ may be obtained from the laws of Biot and Savart, and Lorentz. From the law of Biot and Savart, the magnetic flux B within a conductor of radius R is given by:

$$B = \mu_o I \frac{r^2}{R^2} \tag{2}$$

where $\mu_o$ is the permeability, r is the radial coordinate, and I is the current. From the Lorentz law, the pinch force is given by:

$$\bar{F}_{em} = p_e\bar{E} + \bar{J} \times \bar{B} \tag{3}$$

where $p_e$ is the electrical conductivity, $\bar{E}$ is the electrical field, and $\bar{J}$ is the current density in the electrode. When the liquid drop is spherical and is highly conductive, the approximate longitudinal detaching component of the pinch force is calculated as follows (Ref. 2):

$$F_{em} \sim \int_v (\bar{J} \times \bar{B})\sin\varphi dV \tag{4}$$

$$= \frac{\mu_o I^2}{4\pi}\left[\ln\frac{R_d\sin\Theta}{R} - \left(\frac{1}{4} + \frac{1}{1-\cos\Theta}\right) + \frac{2}{1-\cos\Theta^2}\ln\frac{2}{1+\cos\Theta}\right] \tag{5}$$

where $\Theta$ = the half angle of the arc root (area over which current is transferred from arc to the electrode as shown in Figure 2, $R_d$ is the radius of the drop and R is the electrode radius. As seen from equation 5, the detaching force increases with both increases in the welding current and in the angle of the arc root. However, when the angle of the arc root is very small such that the welding current is converging to a spot, the sign of the force becomes negative and the electromagnetic force acts as a holding force instead of a detaching force.

The drag force on a sphere immersed in a fluid of uniform velocity field at low values of the Reynolds number is obtained as (Ref. 9):

$$F_d = \frac{\pi u^2}{2} P_g R_d^2 C_d \tag{6}$$

where

$$C_d = \frac{6\pi}{N_{Re}} \left[ 1 + \frac{1}{8} N_{Re} \left( 3 + R_1 \right) \right]$$

$$N_{Re} = \frac{R_d u}{v}$$

$$R_1 = \mu_o J^2 \frac{R_d^2}{P_g u^2}$$

where $N_{Re}$ is the Reynolds number, $P_g$ is the density of the gas, and v is the velocity of the gas.

Therefore, the plasma drag force acting on the liquid drop can be approximated by modifying equation (Ref. 6) to allow for the area occupied by the electrode.

The surface tension force, which acts to hold the drops on the electrode is given as follows:

$$F_s = 2\pi R y \tag{7}$$

where y is the surface tension of the liquid metal.

Waszink and Graat (Ref. 11) measured the electromagnetic force in equation 1 and showed good agreement with the calculated results in the globular transfer range.

The pinch instability theory has its origin in the Rayleigh model (Ref. 12) of liquid column instability. Any disturbances to the liquid column tends to activate forces that may cause the liquid column to break up into drops since drops have a lower free energy than the liquid column. The conditions for the liquid column break-up was derived by Rayleigh from the principles of the conservation of mechanical energy of the system. For an inviscid and uncharged system the most probable drop size ($R_o$) created by liquid column disintegration is calculated to be twice the diameter of the liquid column. The pinch instability theory postulates that the pinch force on the liquid column due to the self-induced electromagnetic force enhances the break-up of the liquid column into droplets. An analytical solution of the critical wavelength of this instability in an inviscid jet with current flowing has been derived as (Ref. 13).

$$\lambda_c = \frac{2\pi R}{\left( 1 + \frac{\mu_o I^2}{2\pi^2 R y} \right)^{\frac{1}{2}}} \tag{8}$$

Equation 8 shows that in the presence of an electric current, the critical wave length of the instability of the liquid jet is reduced, leading to a decreased drop size.

The above two theories have been successfully exploited in explaining globular transfer in a qualitative manner, but they are unable to correctly explain spray transfer especially in the streaming transfer mode. Thus, this analysis applies over only a very narrow range of welding parameters which produce projected globular transfer. The specific conditions for which this analysis applies includes: argon shielding gas, steel or aluminum electrodes, constant stick-out, and low welding current. In other cases such as with helium and $CO_2$ shielding gases, metal transfer occurs in a repelled globular transfer mode and the transition to spray transfer is not well defined (Ref. 14). The length of stick-out also has an effect on the mode of metal transfer (Ref. 15). The longer the stick-out, the lower the welding current for spray metal transfer. For Ti-6Al-4V alloy with argon gas shielding, metal transfer always occurs in the repelled globular mode at lower welding currents and in the projected spray mode at high welding currents (Ref. 16).

In addition, as seen in Figure 1, Lesnewich reported a dramatic transition from globular transfer mode to spray transfer mode. In his experiment, as the welding current increases, the drop size and transfer frequency change sharply, marking the transition between globular and spray transfer mode. This phenomena should be reexamined since there are contradicting reports (Refs. 17, 18) which show a smooth rather than a sharp and abrupt transition from globular to spray mode. In any case, this abrupt transition cannot be explained with the static force balance theory and the pinch instability theory. According to these theories the drop size decreases continuously as the welding current increases.

In an attempt to explain the sharp transition in metal transfer mode, Needham et.al. (Ref. 7) proposed that the transition occurs when the plasma envelopes the drop to exert a drag force by the plasma jet, hence the plasma force theory. This theory improves on the static force balance theory in that it explains the transition. Nonetheless, it is without quantitative analysis. The critical velocity theory (Ref. 8) was suggested by analogy with the transition of a liquid column flowing through a cylindrical nozzle in which flow changes from a stream to spray at a critical mass flow rate. Nonetheless, this theory disregards many of the forces on the droplets during welding, such as the electromagnetic force and the plasma drag force.

## 1.2 Heat Flow into the Electrode

With so many theories available and none of comprehensive nature, it is not possible to predict the metal transfer behavior for a wide variety of welding conditions. One of the important reasons lies in the fact that the mass flow and the heat flow are coupled together and previous analyses have treated them separately, thus simplifying the phenomena too much. In the electrode particularly, the metal transfer only occurs after the solid is melted and the coupling between mass flow and heat transfer is very strong.

Heat input into the electrode occurs by several mechanisms, these include electron condensation heating, joule heating and convective heating from the plasma. The electron condensation heat is due to the energy difference between the electrons in the plasma and in the metal. This heat evolves at the location where the electrons condense and, therefore, represents surface rather than bulk heating. Joule heating, which is due to the electrical resistance of the material, is a form of bulk heating and is uniform as long as the current density is uniform. Convective heat transfer from the plasma is another form of surface heating. Depending on the relative intensity of each of these heat sources, the mode of metal transfer may be altered since the geometry of the electrode and the melting rate will be changed.

In this study, the drop size predicted from each theory is calculated and compared with measured results. Also, in an effort to couple the mass flow and the heat flow, the effect of electrode geometry on the metal transfer mode will be physically modeled through a simulation experiment.

## 2.0 EXPERIMENTAL PROCEDURES

The welding power supply used in this study was of the constant current type and can supply DC current with less than 1 percent ripple. The regulator is a transistorized current controller which was designed by Alexander Kusko, Inc. of Needham, Massachusetts, and was constructed in the MIT Welding Laboratory (Ref. 19). The consumable electrode used was mild steel (AWS ER70S-3) of 1.6 mm diameter. The shielding gases used included argon + 2 percent $O_2$ and helium.

To be able to analyze the effect of various heat sources, it is essential to have close control of the stick-out length while measuring drop transfer frequency and drop diameter of the consumable electrode. In this study, a high speed video camera was used with laser back light illumination technique (Ref. 20). With this technique, the stick-out length could be controlled and monitored very precisely during welding. Also, to ensure a relatively constant contact point between the contact tip and the consumable electrode, an alumina tube was inserted into the contact tip leaving only a 5 mm contact length. Figure 3 shows the design of the contact tip used in this experiment.

In another experiment, performed to simulate the plasma drag on the pendant drop, a film of oil was dropped from the end of a tapered metal tip. This experiment was designed to study the effect of electrode geometry on metal transfer. Since it is very hard to independently control the geometry of the welding electrode tip, the apparatus shown in Figure 4 was used to simulate the drop detachment process. Pressurized air was fed into the gas cup providing a detaching force which could be changed by altering the flow rate of air. Tip angles of 15 percent, 30 percent and 60 percent were tested.

# 3.0 RESULTS AND DISCUSSION

## 3.1 Calculation of Equilibrium Drop Size

In a previous study (Ref. 11), the static force balance theory was tested by measuring the magnitude of each of the detaching and the holding forces at a given drop size. This method contains a source of error since the measurements of the forces cannot be made directly under actual welding conditions. Therefore, the forces were measured under simulated conditions to separate each force independently. In this study, rather than measuring the individual forces, the equilibrium drop size was calculated from the theoretical force balance analysis. The advantage of this approach is that the drop size is an easily measurable quantity. At a constant welding current, the sum of the detaching forces and the holding force was calculated for various drop sizes. The equilibrium drop size occurs when the detaching forces and holding force are equal. Figure 5 is an example of one calculation showing the sum of the detaching force as a function of drop size, surface tension holding force and the equilibrium drop size. The data and the assumptions used in the calculation are described in Table 2. By calculating equilibrium drop size at different currents, the equilibrium drop size was determined as a function of current as shown in Figure 6. As seen in the figure, the drop size decreases smoothly as welding current increases and no sharp discontinuity is observed.

The pinch instability theory was also applied using the equation (Ref. 8) shown in Figure 6. The drop size decreases continuously as welding current increases; however, the pinch instability theory predicts drop sizes which are much smaller than the equilibrium drop size predicted by the static force balance theory. At the current range of globular transfer, where the drop size is two to three times the electrode radius, the predicted drop radius is as small as the radius of the electrode.

## 3.2 Drop Size Measurement

Drop size was measured as a function of welding current with two different shielding gases: Ar + 2% $O_2$ and He. The measured drop size using Ar + 2% $O_2$ shielding gas at two different stick-out lengths and the calculated drop size from the static force balance theory and from the pinch instability are plotted in Figure 7. From the definition of the mode of metal transfer, spray transfer occurs at a current of approximately 255 amperes for 26 mm stick-out length and 240 amperes for 33 mm stick-out length. As seen in the figure, the transition from globular to spray mode is smooth and there is no sharp transition. Figure 8 shows the measured frequency of drop transfer. Again, no sign of dramatic transition from globular to spray was observed.

As seen in Figure 7, at a low current level, the predicted drop size from the static force balance is reasonably close to the measured values, but the predicted drop size deviates from the measured values as the welding current increases. The drop size predicted from the pinch instability theory is too small at lower currents and does not tend toward the experimentally determined droplet sizes at high currents.

In Figure 9, the average drop, size which is calculated from the melting rate and the frequency of metal transfer shielded with He gas, is plotted as a function of welding current. The average drop size is calculated rather than measured since the shape of the drop is very irregular causing errors in measurements of drop size. In this case, the decrease in drop size with increased welding current is less than seen with Ar + 2% $O_2$ shielding gas and the large deviation at high welding current is not observed. Nonetheless, the drop size decreases continuously and no sharp transition is seen.

Simple comparison of metal transfer among Ar + 2% $O_2$ and He shielding gases reveals several important differences. First, as stated above, the mode of metal transfer is repelled transfer with He gas as shown in Figure 10 and projected transfer with Ar + 2% $O_2$. The metal transfer mode with He shielding appears to be governed by repelling forces which has not been quantified previously. The pinch instability theory cannot explain this phenomenon.

Second, the current path into the liquid drop changes with different shielding gases. As seen in Figure 10, with Ar + 2% $O_2$, electrons tend to condense all around the liquid drop and onto the solid wall of the cylindrical electrode, which leads to the tapered shape electrode tip at higher welding current; however, with He shielding gas, most of the electrons tend to condense onto the bottom part of the liquid drop and the electrode keeps its cylindrical shape. These phenomena can be rationalized from the fact that the ionization energy of He shielding gas is higher than that of the Ar + 2% $O_2$ gas. Therefore, it is difficult for the electron in He to reach the upper part of the liquid drop and the solid electrode. In this case, there is no heat input onto the surface of the electrode. No side wall melting of the electrode is expected and the electrode will keep its cylindrical shape.

Third, the transition current depends on the stick-out length as Lesnewich observed. This observation is very important in that it suggests that joule heating may affect the metal transfer mode since the stick-out length varies significantly with joule heating. Finally, at higher current ranges when the liquid column emanating from the tapered electrode tip is well developed at streaming transfer mode, a phenomenon which is believed to be a liquid column instability is observed. Figure 11a shows the intact liquid column which later disintegrates into drops by jet instability as in Figure 11b.

By considering the facts that the deviation of the predicted size from measured value is significant with Ar + 2% $O_2$ shielding gas and that the stick-out length which varies temperature of the electrode, affects the deviation also, it is concluded that the deviation may result from melting the side wall of the electrode. The side wall melting has two effects in the static force balance analysis. At first as seen in Figure 12, the vector sum of the holding force of the surface tension will be decreased due to the changing angle of contact. Second, because of the decreased diameter of the drop neck, the total holding force will be decreased from the equation 7.

From the postulation, several important phenomena could be explained and will be discussed at later section. Since the taper is hard to predict through modeling, a simulation experiment was used to evaluate these effects.

## 3.3 Oil Dripping Experiment

Figure 13 shows the measured drop sizes with three different tip angles as a function of gas flow rates. With a 60-degree angle tip, the drop size decreased slightly with increasing gas flow rate, while with a 15-degree angle tip the drop size decreases dramatically with increasing gas flow rate. The drop size change with a 30-degree angle tip is specially interesting in that it shows a transition in droplet detachment mode. At low gas flow rates, the drop forms at the root of the cylindrical electrode as in Figure 14a which corresponds to the first four data points. However, as the gas flow rate increases, the drop starts to form at the tapered corner of the electrode as in Figure 14b and shows a steep decrease in the drop sizes at the high gas flow rates. This is analogous to the metal transfer seen in welding the electrode. This experiment clearly shows that the taper formation at the end of the electrode tip is very crucial in determining the mode of metal transfer.

## 3.4 Comparison Between Static Force Balance Theory and Pinch Instability

The pinch instability theory and static force balance theory have been used in modeling metal transfer, but somewhat disappointing results. Static force balance theory predicted larger drop size than the experimental value. This deviation can be explained by considering the drop movement at the electrode as in Figure 15. Figure 15 is the successive pictures of a pendant drop motion for the 60 milliseconds and it can be seen that the movement of the drop is significant. Therefore, to model the metal transfer more accurately, it is necessary to incorporate the effect of dynamics of drop motion. Picture analyses show that the peak velocity of the pendant drop reaches to 20 cm/sec and the dynamic forces due to the pendant drop movement are approximately calculated to 200 dynes which is enough to account for the deviation of the drop size in the globular mode.

As mentioned in a previous section, the deviation of drop size in spray transfer range could be explained by the taper formation theory combined with static force balance theory. Therefore, to predict the drop size at the spray projected mode, it is necessary to predict the taper and the size of the neck. With the taper formation theory, several important phenomena such as effects of stick-out length and shielding gas on the metal transfer and the transition of metal transfer mode can be explained without difficulties. Transition current decreased with increased stick-out, and the higher temperature of the electrode resulted from increased joule heating. Therefore, the taper can be formed at lower welding current with longer stick-out leading to decreased transition current. Also, the phenomenon that Ar + 2% $O_2$ gas shows the large deviation can be explained by the taper formation theory. Since with Ar + 2% $O_2$ shielding the taper is formed at higher welding currents, the drop size decreases steeply with increased welding currents as in a simulation experiment with a 15-degree tip; however, with He

shielding the taper is not formed, so that the drop size decreases gradually as with the 60-degree tip. Also, the streaming transfer is not expected to occur since the taper is not formed with He shielding.

The drop size predicted from the pinch instability as in equation (8) is unable to match the measured drop size as in Figure 5. One of the fundamental requirements for a pinch instability phenomena to occur is that the liquid metal should be in the form of a cylinder which is at the higher state of free energy than the liquid metal sphere. However, the observation through a high-speed video camera shows that as soon as solid metal melts, it forms a special liquid drop which is at the lower free energy state. Contrary to the postulation of pinch instability, Anno (Ref. 21) predicts that electric charge on the liquid surface has a stabilizing effect, thus, resulting in bigger droplet size. From these observations, it was concluded that pinch instability is not adequate in explaining metal transfer phenomena in globular transfer and spray projected transfer.

When the taper is formed at the electrode at the higher welding currents, as seen in Figure 12, the phenomenon which is believed to be a pinch instability is observed. In this case, the speed of liquid jet is very fast so that the molten metal keeps the cylindrical shape before disintegration. This may explain the plateau of drop size at the high current range of streaming transfer. In this case, the pinch instability theory should be applied to the liquid column which is emanating from the tapered tip of the electrode.

## 4.0 CONCLUSIONS

The metal transfer in the electrode was modeled using pinch instability theory and static force balance theory. The predicted drop size from static force balance theory was reasonably close at globular transfer mode but deviates significantly at spray transfer mode region. At globular transfer mode, the accuracy of the theory can be improved by incorporating the effects of the droplet movements. The deviation at the spray transfer mode is concluded due to the taper formation at the electrode and the simulation experiment proves the effect. Pinch instability theory is unable to explain the metal transfer at globular and spray projected transfer mode, but the drop size at the streaming transfer is thought to be determined by the pinch instability.

The transition of metal transfer mode from globular to spray is observed to be a gradual rather than a sharp and abrupt phenomenon.

## 5.0 ACKNOWLEDGMENT

This work was sponsored by the U. S. Department of Energy under Contract DE-FG02-85ER-13331.

## 6.0 REFERENCES

1. Lesnewich, A., Welding Journal, 37, pp. 418s-425s, 1958.

2. Greene, W.J., TAIEE, part II, pp. 194-203, 1960.

3. Amson, J.C., British Welding Journal, (4), pp. 232-249, 1962.

4. Waszink, J.H. and Gratt, L.H.J., Welding Journal, 62, pp. 109s-116s, 1983.

5. Lancaster, J.F., IIW Document No. 212-429-78.

6. Allum, C.J., J. Phys. D: Appl. Phys., 18, 1147-1468, 1985.

7. Needham, J.C., Cooksey, C.J., and Milner, D.R., British Welding Journal, 7(2), pp. 101-114, 1960.

8. Wasink, J.H. and Van Den Heuvel, G.J.P.M., Welding Journal, pp. 169s-282s, 1982.

9. Sozou, C., J. Fluid Mech., 43(1), pp. 121-127.

10. Rayleigh, L., Proceedings of the Math. Soc., October 4, 1987.

11. Lancaster, J.F., The Physics of Welding, IIW, ed. Pergamon Press, Oxford, pp. 57, 1984.

12. Hazlett, T.B. and Gordon, G.M., Welding Journal, 35, pp. 382s-386s, 1957.

13, Lesnewich, A., Welding Journal, 37, pp. 343s-353s, 1958.

14. Ries, D.E., MS. Thesis, MIT, Cambridge, MA., 1983.

15. Ludwig, H.C., Welding Journal, 36, pp. 25s, 1957.

16. Lancaster, J.F., The Physics of Welding, IIE, ed. Pergamon Press, Oxford, pp. 232, 1984.

17. Eickhoff, S.T., MS Theis, MIT, Cambridge, MA., 1988.

18. Allemand, C.D., Schoeder, R., Ries, D.E. and Eagar, T.W., Welding Journal, 64, pp. 45-47, 1985.

19. Anno, J.N., The Mechanics of Liquid Jets, Lexington Books, Lexington, MA., pp. 5, 1977.

Table 1. IIW Classification of Metal Transfer

| | | |
|---|---|---|
| 1. Free Flight Transfer | | |
| 1.1. Globular | Drop<br>Repelled | low-current GMAW<br>$CO_2$ shielded GMAW |
| 1.2. Spray | Projected<br>Streaming<br>Rotating | Intermediate-current GMA<br>Medium-Current GMA<br>High-Current GMA |
| 2. Bridging Transfer | | |
| 2.1. Short-Circuiting<br>2.2. Bridging without | | Short-Arc GMA<br>Welding with Filler Wire Addition |
| 3. Slag-protected Transfer | | |
| 3.1. Flux-wall Guided<br>3.2. Other Modes | | SAW<br>SAW, Cored Wire, Electroslag |

Table 2. Data used in Static Force Balance analysis

| | |
|---|---|
| Material | steel |
| Electrode Radius (cm) | 0.08 |
| Surface Tension (dyne/cm) | 1800.0 |
| Root Angle (Degree) | 135.0 |
| Gas Velocity (M/sec) | 100.0 |
| Viscosity (cP) | $1.29 \times 10^{-3}$ |

* Current density on the liquid drop is assumed to be uniform.
* The electrode maintains its cylindrical shape.

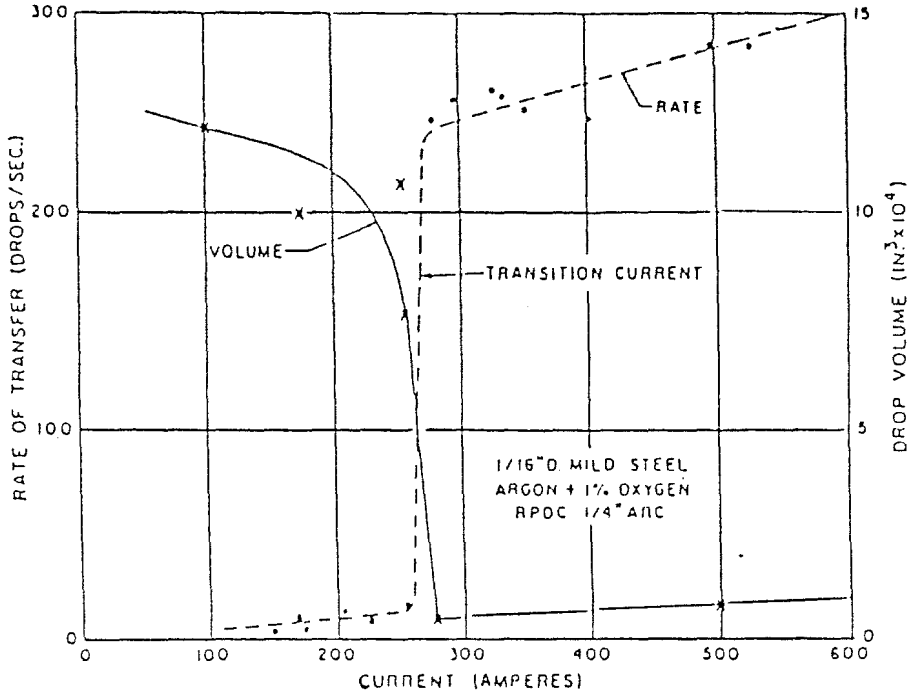


Fig. 1. Effect of current on the size and frequency of drops transferred in an argon-shielded arc.

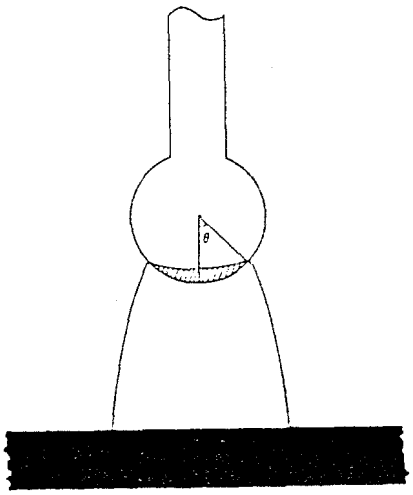


Fig. 2. Definition of the root angle.

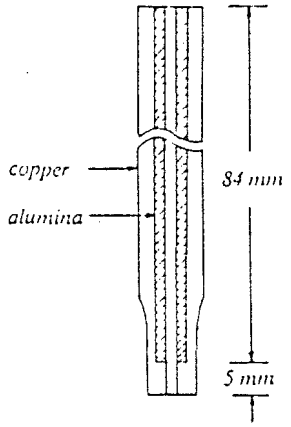


Fig. 3. Contact tip design. An alumina tube is inserted inside of the contact tip so that the actual current contact point is kept constant.

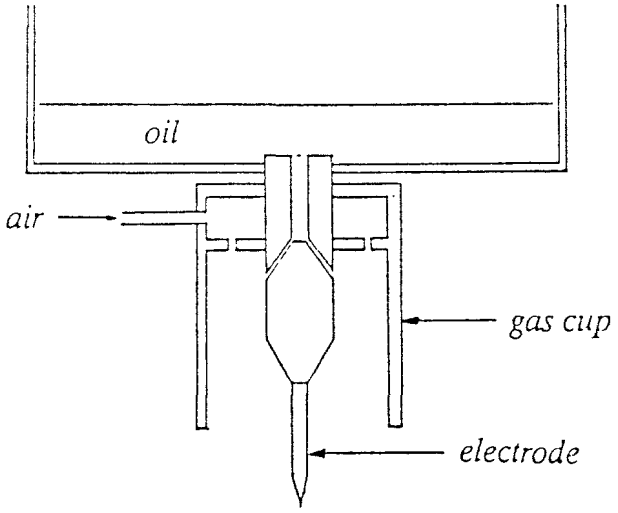


Fig. 4. Oil dripping apparatus

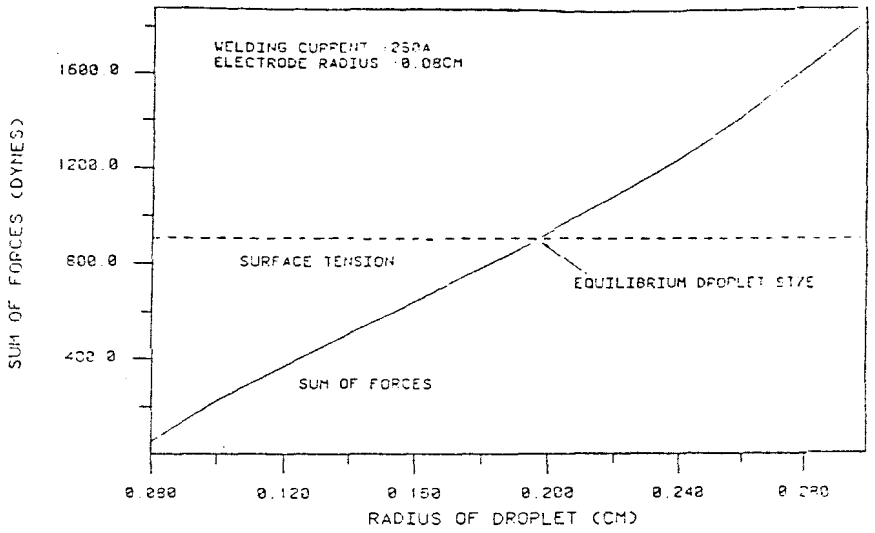


Fig. 5. Static force balance analysis. Equilibrium drop size is the cross-over point where the sum of detaching forces meet the holding surface tension force.

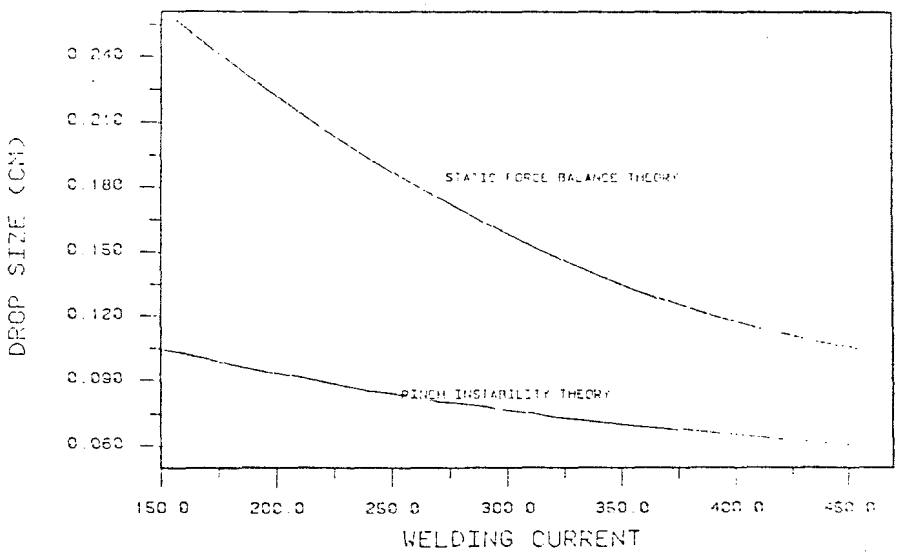


Fig. 6. The predicted drop size from static force balance and pinch instability. The predicted drop size from pinch instability is smaller than from that of static force balance theory.

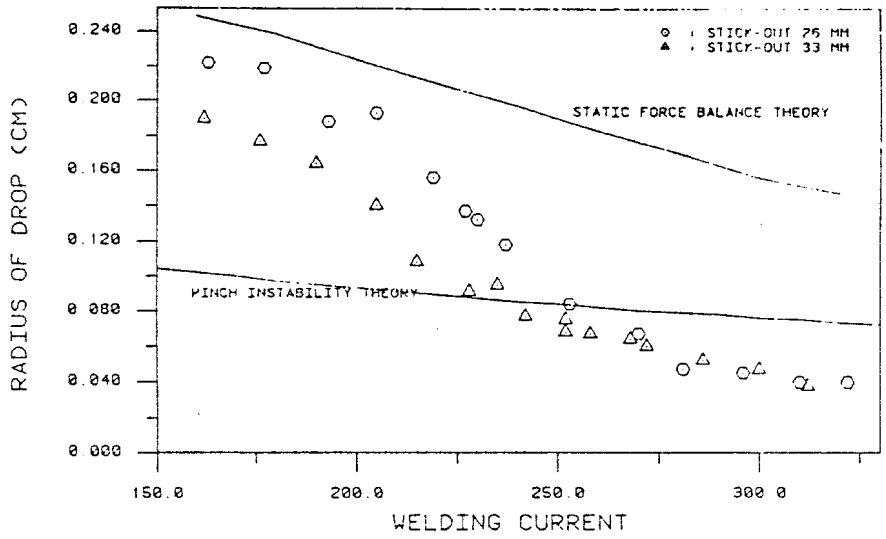


Fig. 7. Comparison of drop size among the predicted and the measured values.

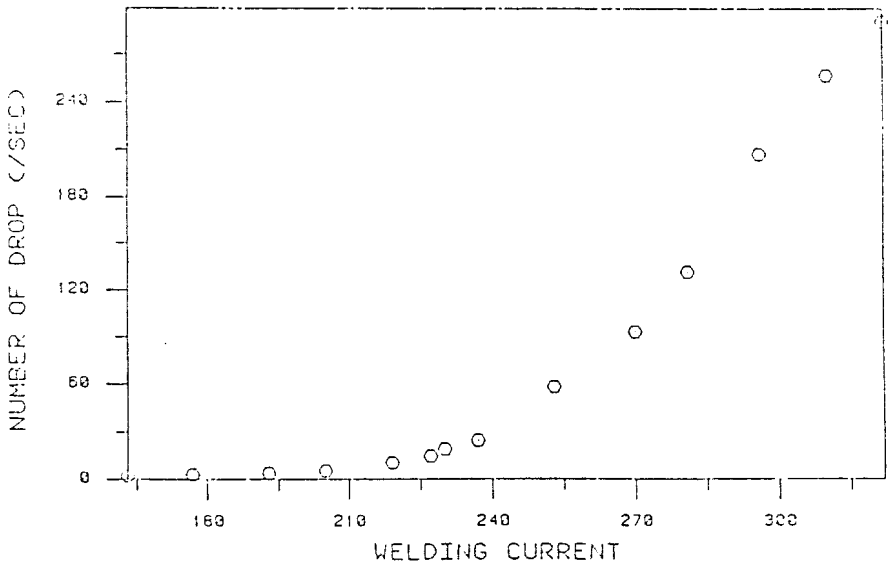


Fig. 8. Frequency of drop transfer with Ar + 2% $O_2$ shielding measured as a function of welding current.

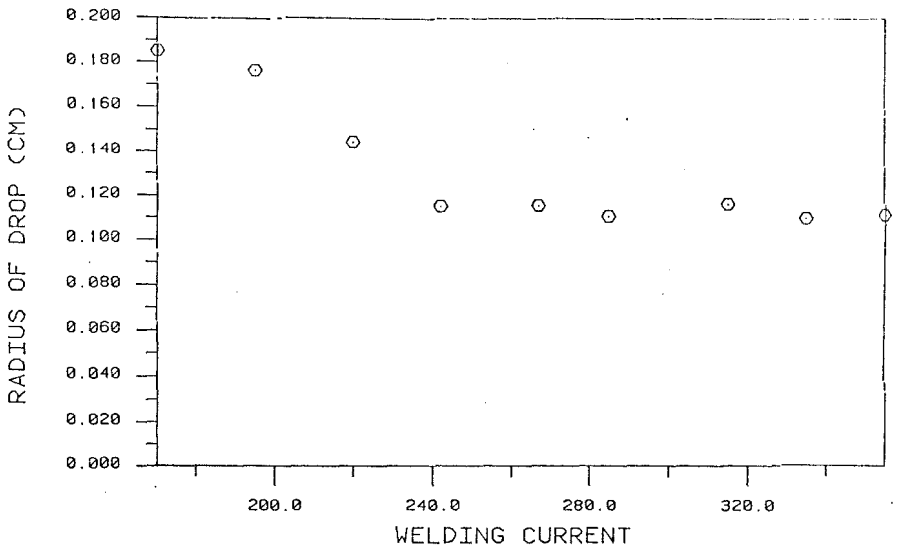


Fig. 9. Variation of drop sizes shielded with He gas as a function of welding current.

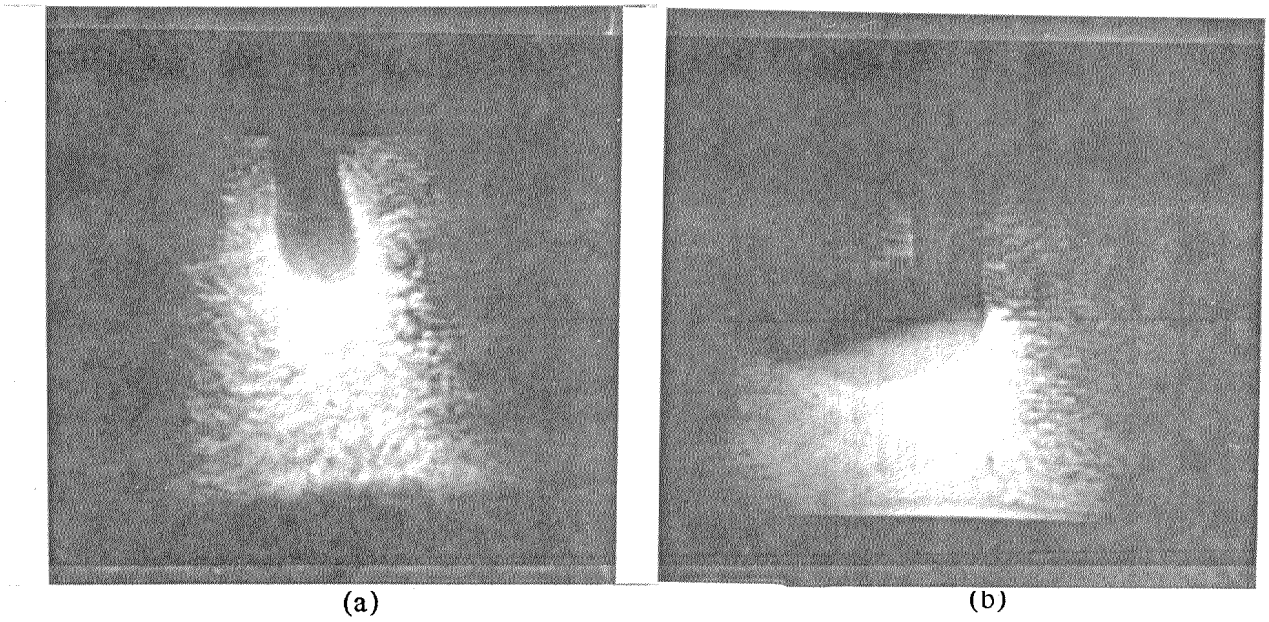


Fig. 10. Typical mode of metal transfer and current path. With Ar + 2%$O_2$ shielding (a) , metal transfer is projected and electrons condense around the drop. With He shielding (b) , repelled transfer is the dominant metal transfer mode and the current path is confined to the bottom of the drop.

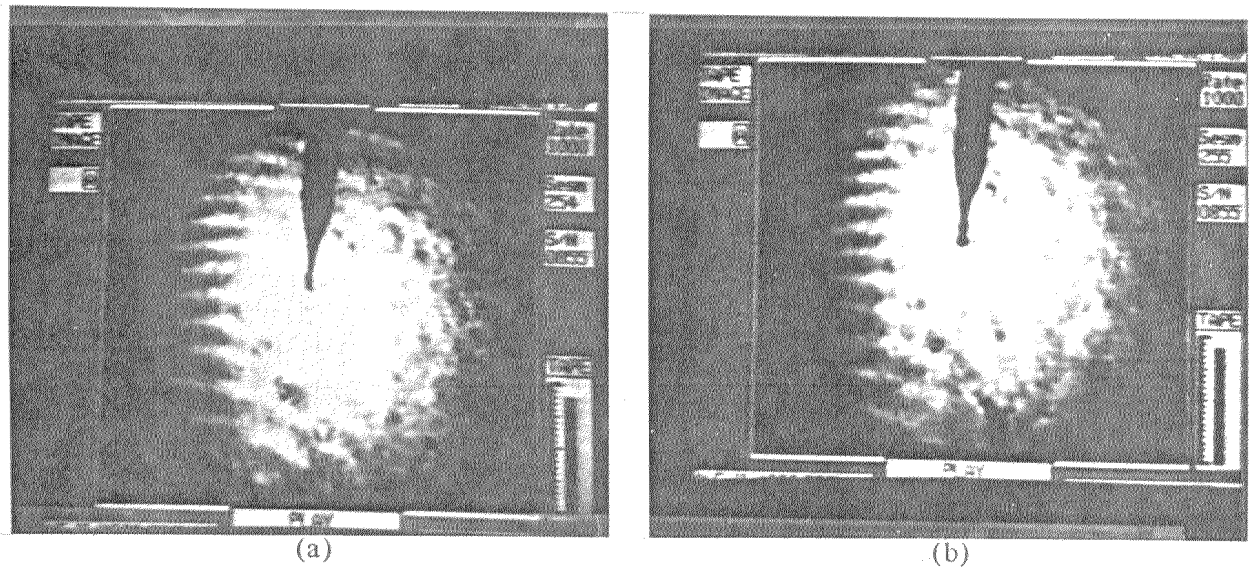


Fig. 11. Streaming metal transfer showing the pinch instability phenomena at the liquid column. (a) shows the intact cylindrical liquid jet and (b) shows the instability of liquid jet after its incubation time.

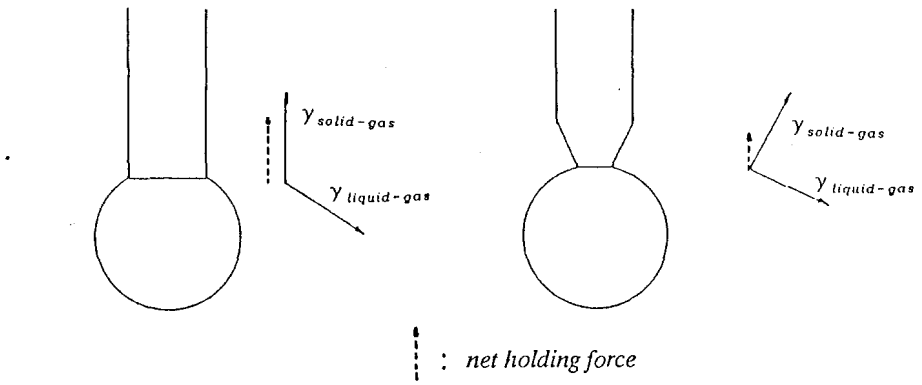


Fig. 12. When the taper is formed at the electrode, there are two sources of reduction in holding forces; reduction of diameter of neck and the vector sum of surface tension.

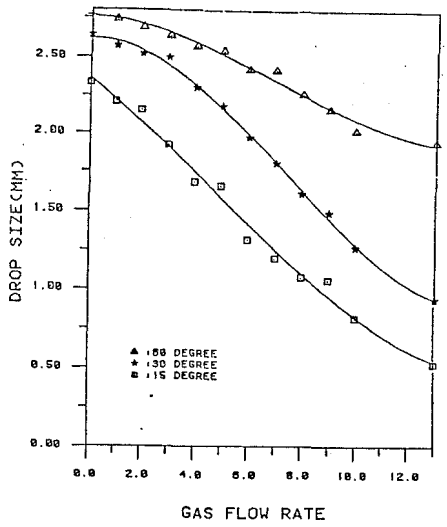


Fig. 13. Drop size measured as a function of gas flow rate (relative scale) in oil dripping apparatus.

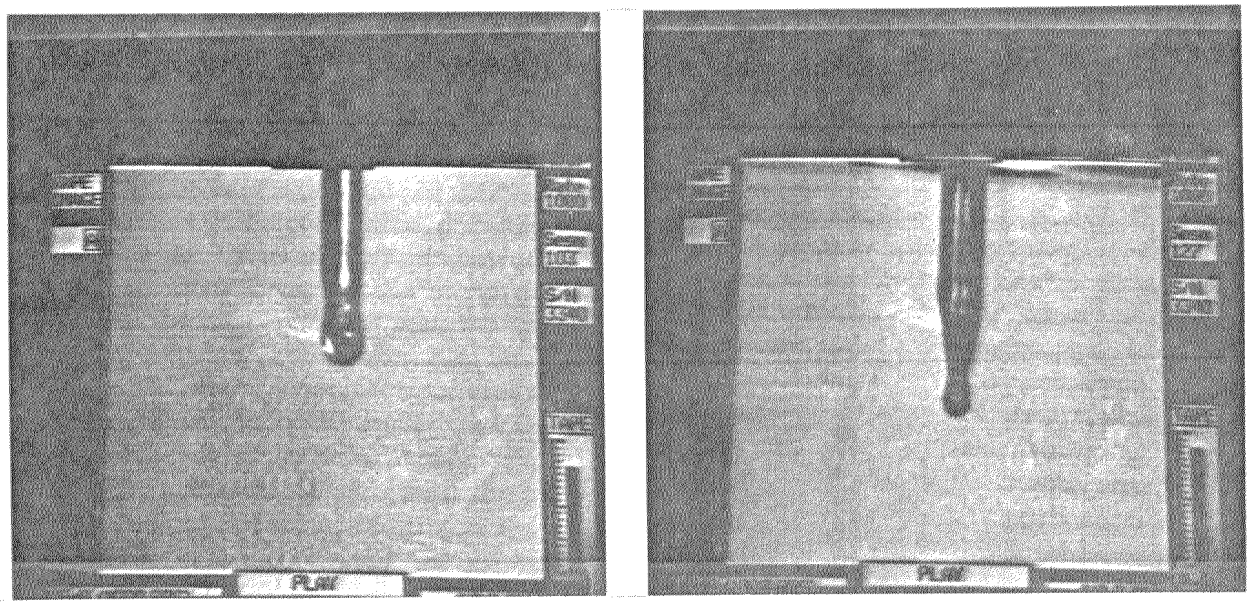

(a) (b)

Fig. 14. Illustration of drop forming position. With low gas flow rate (a), drop forms at the cylindrical part of the electrode and with high gas flow rate (b) drop forms at the end of the taper.

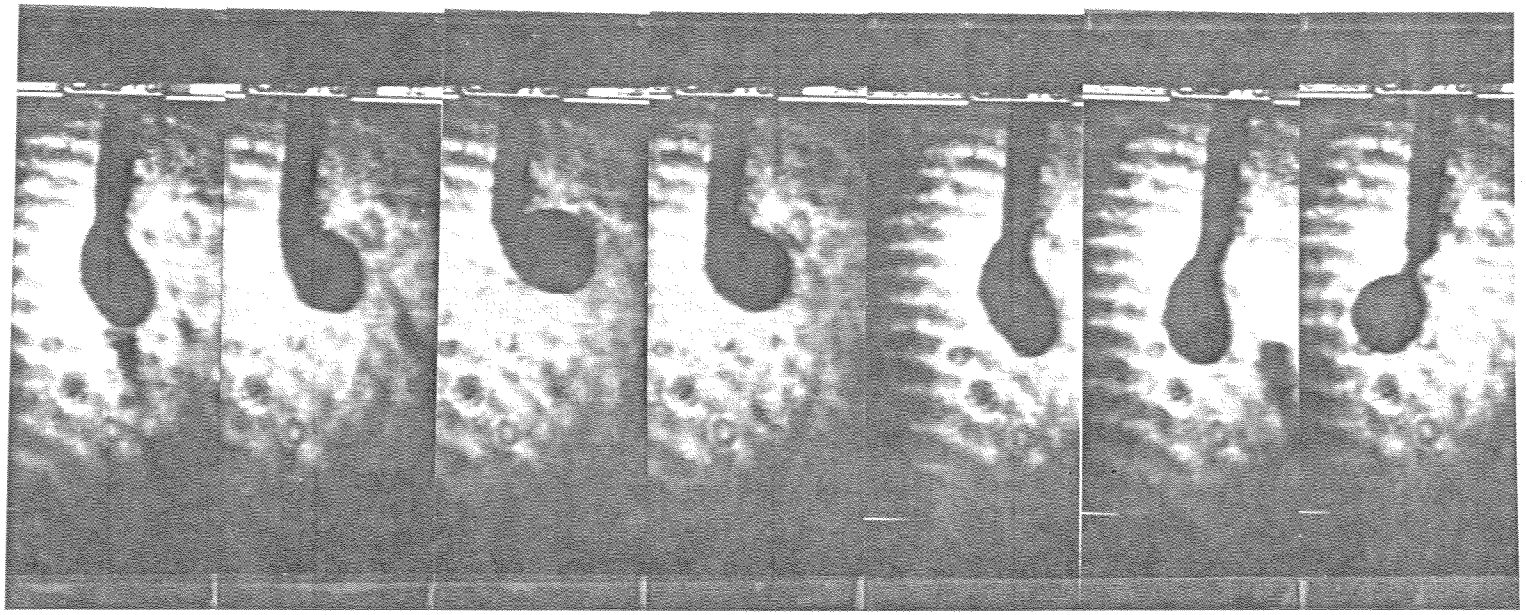

Fig. 15. Successive pictures of a pendent drop motions prior to detach from the electrode (total elaspsed time : 60 milliseconds).